Acoust Aust (2015) 43:275–281
DOI 10.1007/s40857-015-0031-6

ORIGINAL PAPER

Band Structures in Two-Dimensional Phononic Crystals with Periodic S-Shaped Slot

Ting Wang[1,2] · **Mei-ping Sheng**[1] · **Hui Wang**[2] · **Qing-Hua Qin**[2]

Received: 21 August 2015 / Revised: 15 October 2015 / Accepted: 18 October 2015 / Published online: 28 October 2015

Abstract Band structures are investigated in two-dimensional phononic crystals (PC) composed of a periodic S-shaped slot in an air matrix with a square lattice. Dispersion relations, pressure fields and transmission spectra are calculated using the finite element method and Bloch theorem. Numerical results show that the proposed PC can yield complete and large band gaps at lower frequency ranges compared with that of the Jerusalem slots in Li et al. (Phys B 456:261–266, 2015) under the same parameter setting of the lattice and outline of the inclusions. The transmission spectrum is verified to be reasonably consistent with the band gaps along the ΓX direction. By analysing the pressure fields of several modes, the resonance modes of cavities within the S-shaped slot structure are found to result in the low-frequency band gaps. The effects of the geometrical parameters on the upper and lower edges of the first and second complete band gap are further studied. Numerical results show that the bandwidth of the first and second band gaps can be modulated over an extremely large frequency range by the geometrical parameters. The properties of the proposed PC have potential for implementation in structures and devices of noise and vibration control, such as noise filters and waveguides.

Keywords Phononic crystal · Dispersion relation · Transmission spectra · Band gaps

1 Introduction

Much effort has been devoted in recent years to study of the propagation of acoustic/elastic waves in the periodic composites called PCs [1–5]. PCs are artificial media consisting of periodic inclusions in a matrix background with various topologies [6–10]. They can exhibit various special physical properties such as phononic band gaps in which waves are prevented from propagating. The key motivation for proposing new PCs is to explore their potential applications in engineering, such as acoustic filters [11], waveguides [12] and noise insulators [13–15].

According to Ref. [16], the actual formation mechanism of band gaps in PCs remains unobvious, while through the Bragg-scattering mechanism at the Brillouin zone boundaries and through Mie resonances are two typical forms for the band gaps. The mechanism of Bragg-scattering for producing bandgaps is attributed to the destructive interference between incident acoustic waves and reflections from the periodic scatters [17] while the Mie resonance of PCs, being less dependent on periodic scatters, could yield much lower frequency band gaps [18,19].

To achieve low-frequency band gaps, researchers have studied the performance of different PCs. Charles et al. [20] numerically investigated the propagation of guided elastic waves in 2D PCs. They found that Lamb or generalized Lamb modes could stop bands appearing in the dispersion curves. Cui et al. [21] proposed a new PC composed of a square array of parallel steel tubes with narrow slits and analysed the transmissions of the band system. Experimental measurements

✉ Qing-Hua Qin
qinghua.qin@anu.edu.au

[1] School of Marine Science and Technology, Northwestern Polytechnical University, Xi'an 710072, Shaanxi, People's Republic of China

[2] College of Engineering and Computer Science, The Australian National University, Canberra, ACT 2601, Australia

showed that transmission through an array of slit tubes with periodic narrow slits decreased the noise level throughout the frequency interval which is in good agreement with that in the calculated prohibited band. Yu et al. [22] presented a new PC composed of periodic slotted tubes with an internal rib structure in air. Their results showed that the internal rib had a significant influence on the first band gap. Xu et al. [23] investigated the band structures of a two-dimensional solid/air hierarchical PC. Their results showed that the solid/air hierarchical PCs possessed outstanding tuneable band gap features. Gao et al. [24] calculated the dispersion relation, transmission spectra and displacement fields of a two-dimensional PC with two resonators and found that the opening of the bandgaps was due to the local resonance and the scattering interaction between two resonators and matrix. Li et al. [25] presented a band gap structure composed of a periodic Jerusalem cross slot in an air matrix and obtained large band gaps in the low-frequency range.

S-shaped slots are common structures. The band properties of PCs with S-shaped inclusions have yet not been reported, as far as we know. In this paper, band structures of a novel two-dimensional PC with an S-shaped slot are evaluated using the finite element method (FEM) [10,22,25–27]. The formation mechanisms of bands are analysed based on the acoustic mode. The transmission spectra of the S-shaped structure are also investigated. Further, the effects of the geometric parameter on the first and second complete band gap are discussed. Compared with the Jerusalem cross slot and internal rib structure, the S-shaped structure could achieve comparable or even superior results with simpler configuration for manufacturing.

2 Model and Methods of Calculation

A two-dimensional PC with an S-shaped slot in an air matrix of a square lattice is considered (see Fig. 1). Figure 1a and b show schematic views of the cross-section of the proposed PC structure and the representative unit cell. The parameters of the unit cell including the S-shaped slot are defined as follows: the cell length of the square lattice is a, and m and n are, respectively, the vertical parameters shown in Fig. 1b. The horizontal length of the S-shaped slot is l. The width of the slot is assumed to be d. By repeating the representative unit cell along the x and y directions, an infinite two-dimensional PC is formed. In the following calculation, the lattice constant $a = 36$ mm and the slot width $d = 2$ mm are used.

To investigate the acoustic band gaps and eigenmodes of the proposed structure, calculations of the dispersion relations and transmission spectra are conducted using the FEM and the Bloch theorem. Since the infinite system is periodic along the x and y directions simultaneously, only the representative unit cell in Fig. 1b needs to be considered. In the calculations, the representative unit cell is divided into two domains, the fluid domain and the solid domain. For the fluid domain, the governing equation of the acoustic waves can be given by the Helmholtz equation in frequency domain as follows.

$$\nabla\left(-\frac{1}{\rho_0}\nabla p\right) = \frac{\omega^2 p}{\rho_0 c_s}, \tag{1}$$

where p, ρ_0, ω and c_s are the acoustic pressure, density, angular frequency and speed of the fluid, respectively.

As the acoustic impedance of air is much lower than that of the solid, longitudinal waves propagating in the air will be reflected by the S-shaped inclusions. Therefore, the wave propagation in the air domain is predominant, and the transverse waves in solid inclusions can be neglected. The solid S-shaped inclusions are considered as fluid with very high stiffness and specific mass. The periodic conditions applied at the boundaries between the representative unit cell and its four adjacent cells are:

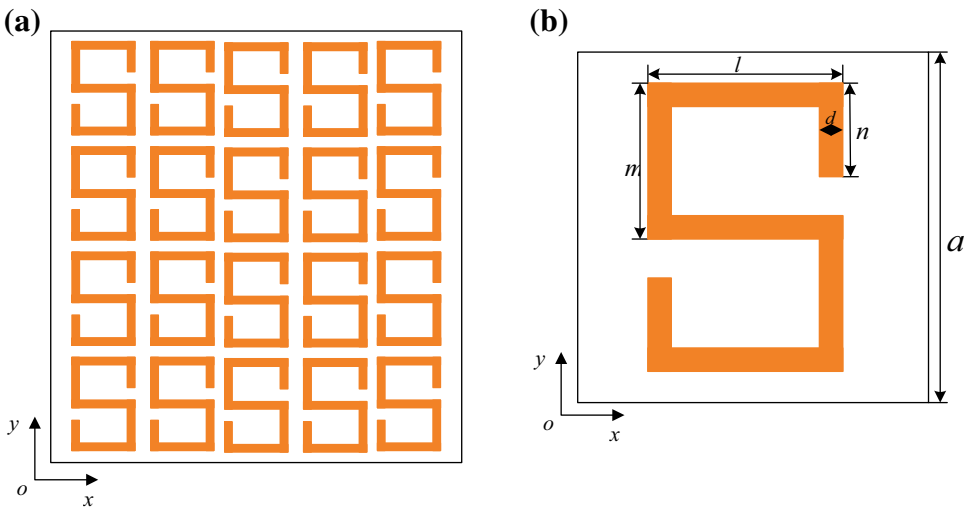

Fig. 1 **a** Schematic view of the cross-section of the two-dimensional PC. **b** The representative unit cell of the proposed PC

$$p\left(\mathbf{r}+\mathbf{a}\right)=p\left(\mathbf{r}\right)e^{i\mathbf{k}\bullet\mathbf{a}}, \tag{2}$$

where $\mathbf{r}$ is located at the boundary nodes and $\mathbf{a}$ represents the basis vector of the periodic structure. $\mathbf{K}$ is defined as a two-dimensional Bloch wave vector. We solve the eigenvalue equations with the software COMSOL Multiphysics 4.3b. The acoustic module operates under a two-dimensional pressure acoustic application mode (acpr). A constant boundary condition is applied to the boundaries between the air and the solid, and a periodic boundary condition is imposed on the two opposite boundaries of the representative unit cell. The triangular mesh with Lagrange quadratic elements provided by COMSOL is used to discretise the unit cell. Eigenfrequency analysis is chosen as the solving mode and the direct (MUSR) is applied as the linear system solver. A group of corresponding eigenfrequencies and eigenmodes can be obtained with a given value of the Bloch wave vector $\mathbf{K}$. By changing the values along the boundaries of the first Brillouin zone and repeating the calculation, the dispersion relations of the proposed PC can be obtained.

For the calculation of transmission spectra, we consider a finite element system composed of 16 representative units in x direction with a periodic condition imposed on y direction to represent the infinite system. Boundaries between the air and the S-shaped inclusions can still be treated as constant boundaries because of the high stiffness and specific mass of the slot. The governing equation for the acoustic waves is the same as Eq. (2). Radiation boundary conditions which allow an outgoing wave to leave the solution domain with minimal reflections are applied to the left and right boundaries of the finite system, yielding

$$\begin{aligned}&\mathbf{n}\bullet\left(\frac{1}{\rho_0}\nabla p\right)+i\frac{k}{\rho_0}p+\frac{i}{2k}\Delta_T p\\&=\left(\frac{i}{2k}\Delta_T p_0+\left(ik-i\left(\mathbf{K}\bullet\mathbf{n}\right)\frac{p_0}{\rho_0}\right)\right)e^{-i(\mathbf{kr})}\\&\quad\times\mathbf{K}=-k\mathbf{n},\end{aligned} \tag{3}$$

where p is the pressure, $\mathbf{n}$ is the inward normal vector of the structure, k is the wave number, Δ_T represents the Laplace operator in the tangent plane at certain point on the boundary and p_0 is the amplitude of the plane wave of the sound source. The sound source is located on the left boundary with $p_0 = 1$ Pa. The plane waves with single frequencies travel from the left side to the right side along x direction. The transmission spectra are defined as

$$TL=10\log_{10}\left(\frac{P_{\text{in}}}{P_{\text{out}}}\right), \tag{4}$$

where P_{in} and P_{out} denote incident power on the left side and transmitted power on the right side of the finite system, respectively. By varying the excitation frequency of the incident waves, the transmission spectra are obtained.

3 Results and Discussion

3.1 Band Gaps of the Proposed PCs with Periodic S-Shaped Slot

Some numerical results are given in Fig. 2 to illustrate the characteristics of the band gaps in the proposed PC structure. Since the inclusion is out of 90-degree symmetry, the wave vector should sweep the edge of the irreducible Brillouin

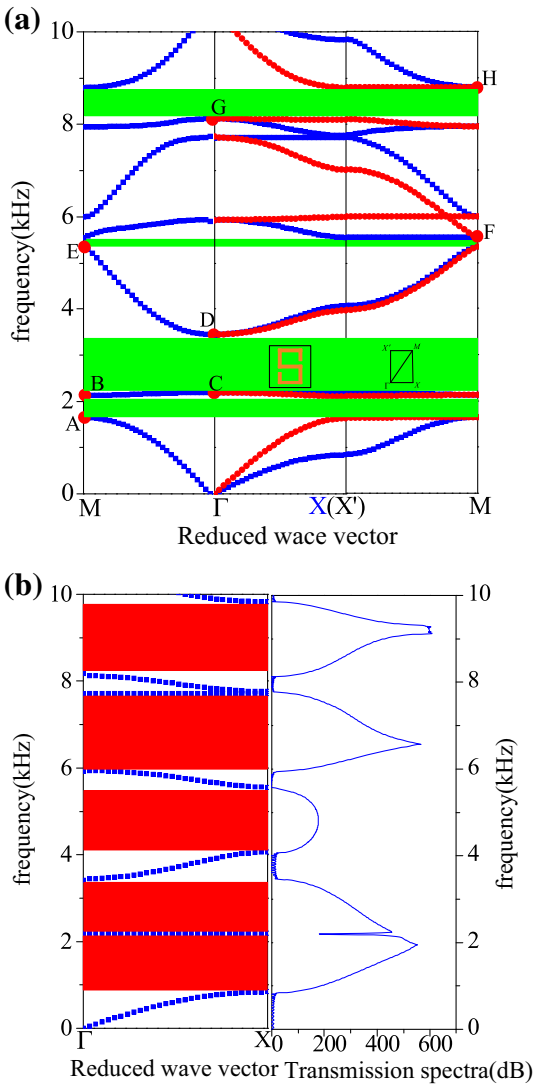

Fig. 2 **a** Band structure in the proposed PC composed of a periodic square array of S-shaped slots in an air matrix. The unit cell and the first Brillouin zone are shown in the second band gap. **b** The band structure along $\Gamma - X$ direction and transmission spectra in $\Gamma - X$ direction of a finite structure composed of 16×1 unit cells

zone, along a rectangular boundary. The material parameters are chosen as follows: density $\rho_0 = 7850$ kg/m^3 and sound speed of the longitudinal wave $c_{s0} = 6100$ m/s for steel; $\rho_1 = 1.25$ kg/m^3 and $c_{s0} = 343$ m/s for air. The geometric parameters of a typical representative cell are defined as: lattice constant $a = 36$ mm, vertical slot length $m = 14$ mm and $n = 8$ mm, horizontal slot length $l = 28$ mm and slot width $d = 2$ mm.

Figure 2a shows the band structure of the PC with several complete band gaps and orientational band gaps from 0 to 10 kHz in which seven bands, including four complete band gaps (green regions) and five wider orientational band gaps (red regions along the ΓX direction in Fig. 2b) are involved. The lowest complete band gap, between the first band and the second band, extends from 1647 to 2124 Hz, which is nearly 200 Hz lower than that of the Jerusalem inclusion mentioned in Ref. [25] with the same lattice constants, vertical and horizontal length of the inclusions and the width of the slot, thus is more suitable for lower frequency noise control. The other three band gaps extend from 2189 to 3445 Hz for the second complete band gap (between the second and third band) which is 840 Hz lower than that of the Jerusalem configuration, from 5341 to 5554 Hz for the third band gap (between the third and fourth band), and from 8096 to 8796 Hz for the fourth band gap (between the sixth and seventh band), respectively. The widths of the complete band gaps are, respectively, 447, 1256, 213 and 700 Hz. All these complete band gaps are very useful for sound control because they could prohibit the propagation of waves irrespective of direction through the two-dimensional PC. It also can be seen that the gap widths of the orientational band gaps are much wider than those of the complete band gaps. The advantage of the orientational band gaps can be taken for preventing waves propagating from a specific direction.

In order to validate the characteristics of the band structure of the proposed PC, transmission spectra are computed using FEM. Figure 2b demonstrates the calculated transmission spectra for plane acoustic waves propagating in the proposed PC along x direction of the finite PC structure with 16×1 unit cells corresponding to the $\Gamma - X$ direction of the unit cell. It can be seen that large attenuations in four frequency ranges emerge in the transmission spectra from the right figure in Fig. 2b, which shows good agreement with the orientational band gaps in the left figure in Fig. 2b.

It can be observed in Fig. 2a that some bands are flat in most of the range in the first Brillouin zone, namely the first, second, fourth and sixth bands, which may mean that some localized resonant modes exist in this PC structure. As such, we investigate the distribution of the acoustic pressure field at some specific points of the band structure to obtain deeper understanding of the formation mechanism of the bandgaps. The acoustic modes at the points marked as A, B, C, D, E, F, G and H in Fig. 2a are illustrated in Fig. 3.

Figure 3a shows that the acoustic pressure field of mode A mainly concentrates in the two cavities of the S-shaped slot structure with opposite phases. Compared with the pressure within the cavities, the pressure field outside is so small that it can be ignored. The two cavities act as resonators. From Fig. 3b, we can see that the resonances of the two cavities are in the same phase and the minimum pressure concentrates on the two corners of the unit cell. The pressure field of mode C is opposite to that of mode A and with greater pressure. The resonance of the two cavities dissipates most of the energy of the unit cell. Comparing mode D with mode B, it can be observed that the main difference is the location of the minimum pressure which mainly distributed on the upper and lower sides of the S-shaped inclusion. The energy in the four modes from A to D is concentrated on the two cavities within the S-shaped slot. It can be concluded that the first and second band gaps are mainly attributed to the resonance of the two cavities within the S-shaped slot and can be modulated by changing the geometric parameters of the S-shaped inclusion to alter the cavities.

Figure 3e demonstrates that the pressure field of mode E is almost concentrated on the two closed corners outside the cavities and the pressure within the cavities is nearly zero. This indicates that the lower edge of the third band gap is mostly related to the external structure and changing the geometric parameters of the inclusion has little effect on the band gap. For mode F in Fig. 3f, the pressure field is similar to that of mode E but with different locations of the maximum and minimum pressure which are located at the upper and lower sides of the S-shaped inclusion. Thus the upper edge of the third band gap bears little relationship to the geometric parameter of the inclusions. For modes G and H, it can be observed that resonance occurs in the two cavities, with each cavity including two reversed phase resonances. From mode E to mode H, it can be seen that the pressure field is distributed within and outside the inclusion. When the pressure field is concentrated on the outside, the pressure outside is much greater than that inside. On the other hand, when the pressure field is concentrated on the inside, the pressure within is much greater than that outside. It can, therefore, be concluded that the third band gap is produced by the interaction of acoustic pressure fields within and outside the S-shaped slot and the slot has little effect on the band gap, whereas the fourth band gap is mainly attributed to the resonance within the cavities and the gap width can be modulated by the geometric parameters.

3.2 Effects of Geometric Parameters on the First and Second Band Gaps

It is noted that the geometric parameters have significant influences on band gaps of the proposed PC. The lower the frequency of the acoustic wave is, the longer the wavelength

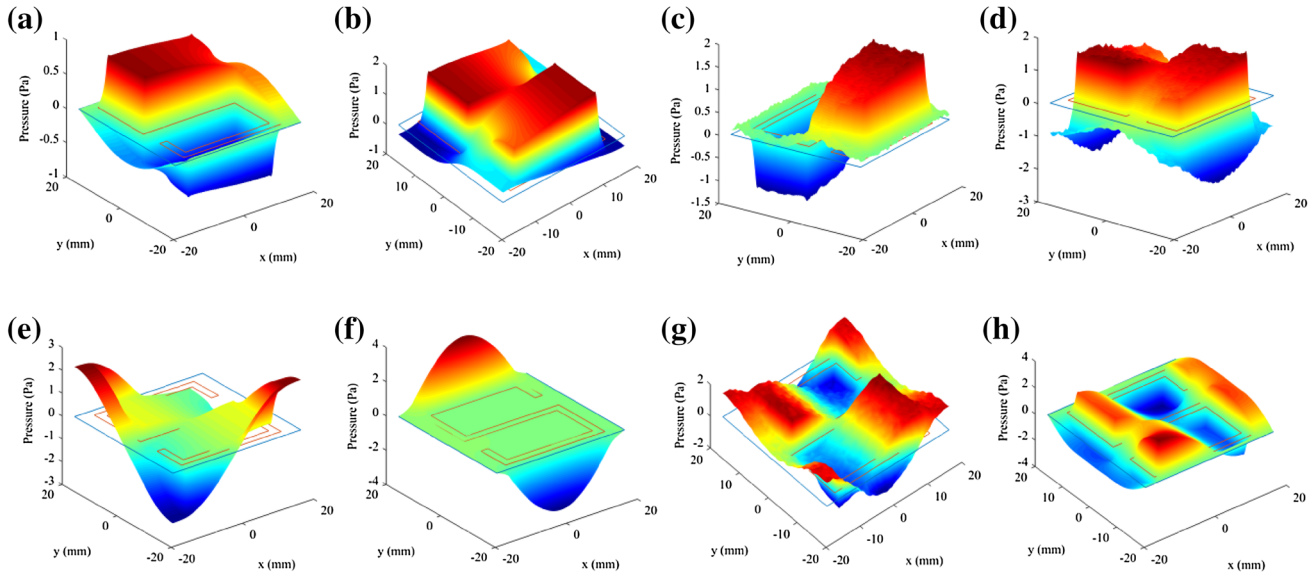

Fig. 3 Pressure field at a representative unit cell of the eigenmodes marked A (**a**), B (**b**), C (**c**), D (**d**), E (**e**), F (**f**), G (**g**) and H (**h**) in Fig. 2a

is and the more difficult the noise control is. Moreover, the acoustic pressure fields of mode A, B and C indicates the edges of the first and second band gaps are related to the resonance of the two cavities which are dependent on the geometry parameters. For this reason, the effects of the geometric parameters are taken into consideration mainly on the first and second band gaps. In the analysis, the band gaps are irrespective of direction, which means phonon cannot pass through the PC.

Figure 4 shows trends of the first and second band gaps with edges as a function of the horizontal length of the slot l. The shaded zones with oblique blue and red lines represent the widths of the first and second band gaps, respectively. In our analysis, the slot width $d = 2$ mm, vertical length $m = 14$ mm and $n = 8$ mm are kept the same. We can see that with the increase of the horizontal length of the slot l, edges of both of the band gaps shift to a lower frequency range, and the slopes of the upper edge of the first band gap and the lower edge of the second band gap are approximately same, which results in the gap between the two band gaps unchanged. While the widths of both band gaps are getting slightly wider as the horizontal length becomes larger. With the analysis of the effects of the horizontal length of the slot l on the band gaps, it can be concluded that a longer l could push the first and second band gaps to lower frequency ranges with the gap width slightly changed, which is helpful for lower noise control.

In order to investigate the effect of the vertical length of the slot m, the band structures of the proposed PCs are calculated with different values of m ranging from 9 to 14 mm. In the process of calculation, the slot width $d = 2$ mm, the vertical length $n = 8$ mm and the horizontal length $l = 28$ mm are

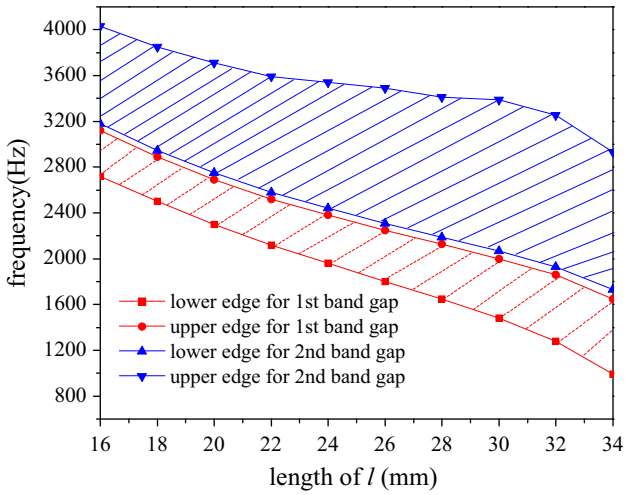

Fig. 4 Effect of the central length of the slot l on the first and second band gaps with the slot width $d = 2$ mm, *vertical length* $m = 14$ mm and *vertical length* $n = 8$ mm

kept constant. Figure 5 illustrates the changes of the first and second band gaps as a function of the vertical length of the slot m. It can be observed that as the length of m increases, the second band gap moves to a higher frequency range, simultaneously the gap width broadened, while the lower edge of the first band gap fluctuates as m changes, leading to uncertain gap width. The fluctuation of the first band gap gets more severe with lager m. That means, the vertical length of the slot m could modulate the location and position of the first and second band gaps flexibly when brought into applications.

The effects of another vertical lengths of the slot n on the first and second band gaps are shown in Fig. 6 with the slot

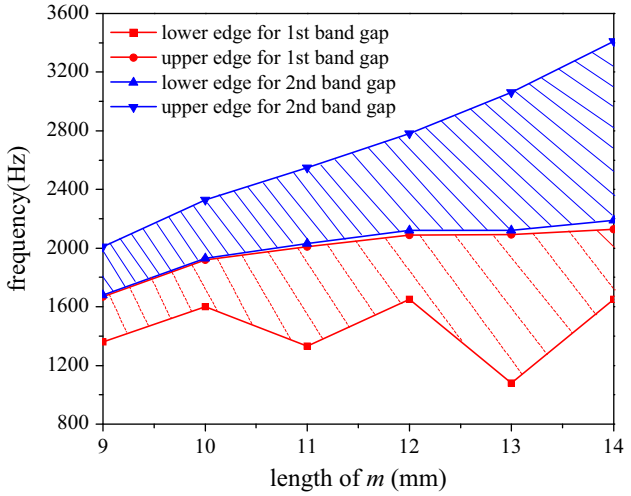

Fig. 5 Effect of the *vertical length* of the slot m on the first and second band gaps with the slot width $d = 2$ mm, *horizontal length* $l = 28$ mm and *vertical length* $n = 8$ mm

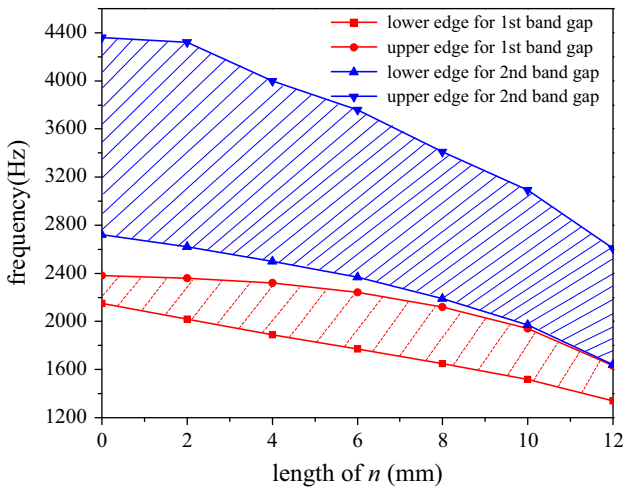

Fig. 6 Effect of the side length of the slot n on the first and second band gaps with the slot width $d = 2$ mm, *horizontal length* $l = 28$ mm and *vertical length* $m = 14$ mm

values of width $d = 2$ mm, vertical length $m = 14$ mm and horizontal length $l = 28$ mm unchanged during the calculation while n varying from 0 to 12 mm at a step of 2 mm. It can be seen that, with the increase of the vertical length n, both of the band gaps move to a lower frequency range; the width of the second band gap gets narrower while the shape of the first band gap resembles a spindle. Consequently, the gap between the two band gaps gets narrower which hints a merge of the two band gaps into a wider one in lower frequency ranges. The results above indicate that the vertical length n has a much greater influence on the first and second band gaps.

From the analysis of the parameters effect on the first and second band gaps, conclusions can be drawn that each length of the inclusion slot could modulate the band gaps in different ways. The horizontal length l could push the two band gaps to lower frequency ranges with slightly broadening their width. The vertical length n can also lower the location of the two band gaps, while narrower gap widths. Changing of the vertical length of m may broaden the second band gap in higher frequency ranges.

4 Conclusions

Making use of the FEM and the Bloch theorem, we investigated the band structures of a two-dimensional PC composed of periodic S-shaped inclusions in an air matrix of a square lattice. Numerical results show that the proposed PC can generate several complete band gaps and induce wider orientational band gaps than existing PCs. Transmission spectra are also calculated, and the results show reasonable consistency with the orientational band gaps along the ΓX direction. Pressure fields are analysed to achieve better understanding of the formation mechanism of band gaps and it shows the lower band gaps are because of resonance in the cavities which are strongly dependent on the geometry parameters. Furthermore, the effects of geometric parameters on the first and second band gaps are investigated. It can be concluded that the gap width can be tuned over a very large frequency range by geometric parameters such as the vertical length and the horizontal length of the S-shaped slot. With these properties, the proposed PC could be implemented in engineering applications such as sound insulation and noise filtering.

Acknowledgments The first author gratefully acknowledges the financial support of the China Scholarship Council.

References

1. Hirsekorn, M.: Small-size sonic crystals with strong attenuation bands in the audible frequency range. Appl. Phys. Lett. **84**, 3364–3366 (2004)
2. Qiu, C., Liu, Z., Shi, J., Chan, C.T.: Directional acoustic source based on the resonant cavity of two-dimensional phononic crystals. Appl. Phys. Lett. **86**, 224105 (2005)
3. Mohammadi, S., Eftekhar, A.A., Khelif, A., Hunt, W.D., Adibi, A.: Evidence of large high frequency complete phononic band gaps in silicon phononic crystal plates. Appl. Phys. Lett. **92**, 221905 (2008)
4. Wu, T.-T., Chen, Y.-T., Sun, J.-H., Lin, S.-C.S., Huang, T.J.: Focusing of the lowest antisymmetric Lamb wave in a gradient-index phononic crystal plate. Appl. Phys. Lett. **98**, 171911 (2011)
5. Leamy, M.J.: Exact wave-based Bloch analysis procedure for investigating wave propagation in two-dimensional periodic lattices. J. Sound. Vib. **331**, 1580–1596 (2012)
6. Larabi, H., Pennec, Y., Djafari-Rouhani, B., Vasseur, J.O.: Multicoaxial cylindrical inclusions in locally resonant phononic crystals. Phys. Rev. E **75**, 066601 (2007)

7. Pennec, Y., Djafari-Rouhani, B., Vasseur, J.O., Khelif, A., Deymier, P.A.: Tunable filtering and demultiplexing in phononic crystals with hollow cylinders. Phys. Rev. E **69**, 046608 (2004)
8. Vasseur, J.O., Morvan, B., Tinel, A., Swinteck, N., Hladky-Hennion, A.C., Deymier, P.A.: Experimental evidence of zero-angle refraction and acoustic wave-phase control in a two-dimensional solid/solid phononic crystal. Phys. Rev. B **86**, 134305 (2012)
9. Lai, Y., Wu, Y., Sheng, P., Zhang, Z.-Q.: Hybrid elastic solids. Nat Mater. **10**, 620–624 (2011)
10. Yu, K., Chen, T., Wang, X.: Large band gaps in two-dimensional phononic crystals with neck structures. J. Appl. Phys. **113**, 134901 (2013)
11. Qiu, C., Liu, Z., Mei, J., Shi, J.: Mode-selecting acoustic filter by using resonant tunneling of two-dimensional double phononic crystals. Appl. Phys. Lett. **87**, 104101 (2005)
12. Khelif, A., Choujaa, A., Benchabane, S., Djafari-Rouhani, B., Laude, V.: Guiding and bending of acoustic waves in highly confined phononic crystal waveguides. Appl. Phys. Lett. **84**, 4400–4402 (2004)
13. Lee, C.-Y., Leamy, M.J., Nadler, J.H.: Frequency band structure and absorption predictions for multi-periodic acoustic composites. J. Sound Vib. **329**, 1809–1822 (2010)
14. Xiao, Y., Wen, J., Wen, X.: Sound transmission loss of metamaterial-based thin plates with multiple subwavelength arrays of attached resonators. J. Sound Vib. **331**, 5408–5423 (2012)
15. Xiao, Y., Wen, J., Yu, D., Wen, X.: Flexural wave propagation in beams with periodically attached vibration absorbers: band-gap behavior and band formation mechanisms. J. Sound Vib. **332**, 867–893 (2013)
16. Yudistira, D., Boes, A., Djafari-Rouhani, B., Pennec, Y., Yeo, L.Y., Mitchell, A., Friend, J.R.: Monolithic phononic crystals with a surface acoustic band gap from surface Phonon-Polariton coupling. Phys. Rev. Lett. **113**, 215503 (2014)
17. Tanaka, Y., Tomoyasu, Y., Tamura, S.I.: Band structure of acoustic waves in phononic lattices: two-dimensional composites with large acoustic mismatch. Phys. Rev. B **62**, 7387–7392 (2000)
18. Liu, Z., Zhang, X., Mao, Y., Zhu, Y.Y., Yang, Z., Chan, C.T., Sheng, P.: Locally resonant sonic materials. Science **289**, 1734–1736 (2000)
19. Wang, G., Wen, X., Wen, J., Shao, L., Liu, Y.: Two-dimensional locally resonant phononic crystals with binary structures. Phys. Rev. Lett. **93**, 154302 (2004)
20. Charles, C., Bonello, B., Ganot, F.: Propagation of guided elastic waves in 2D phononic crystals. Ultrasonics **44**, e1209–e1213 (2006)
21. Cui, Z.Y., Chen, T.N., Chen, H.L., Su, Y.P.: Experimental and calculated research on a large band gap constituting of tubes with periodic narrow slits. Appl. Acoust. **70**, 1087–1093 (2009)
22. Yu, K.P., Chen, T.N., Wang, X.P., Zhou, A.A.: Effect of the internal rib structure of the inclusions on the two-dimensional phononic crystal composed of periodic slotted tubes in air. Phys. B **407**, 4287–4292 (2012)
23. Xu, Y.L., Tian, X.G., Chen, C.Q.: Band structures of two dimensional solid/air hierarchical phononic crystals. Phys. B **407**, 1995–2001 (2012)
24. Gao, N., Wu, J.H., Yu, L.: Research on bandgaps in two-dimensional phononic crystal with two resonators. Ultrasonics **56**, 287–293 (2015)
25. Li, Y., Chen, T., Wang, X., Yu, K., Song, R.: Band structures in two-dimensional phononic crystals with periodic Jerusalem cross slot. Phys. B **456**, 261–266 (2015)
26. Qin, Q.-H.: Trefftz finite element method and its applications. Appl. Mech. Rev. **58**, 316–337 (2005)
27. Qin, Q.H.: The Trefftz finite and boundary element method. WIT Press, Southampton (2000)